



**HAL**  
open science

## Seasonal and interannual variations of suspended particulate matter in a West-African lagoon (Nokoué lagoon, Benin): Impact of rivers and wind

Indrig Laeticia Ntangyong, Alexis Chaigneau, Yves Morel, Arnaud Assogba, Victor Olaègbè Okpeitcha, Thomas Duhaut, Thomas Stieglitz, Pieter van Beek, Ezinvi Baloitcha, Zacharie Sohoun, et al.

### ► To cite this version:

Indrig Laeticia Ntangyong, Alexis Chaigneau, Yves Morel, Arnaud Assogba, Victor Olaègbè Okpeitcha, et al.. Seasonal and interannual variations of suspended particulate matter in a West-African lagoon (Nokoué lagoon, Benin): Impact of rivers and wind. *Estuarine, Coastal and Shelf Science*, 2024, 304, pp.108821. 10.1016/j.ecss.2024.108821 . hal-04608784

**HAL Id: hal-04608784**

**<https://hal.science/hal-04608784>**

Submitted on 11 Jun 2024

**HAL** is a multi-disciplinary open access archive for the deposit and dissemination of scientific research documents, whether they are published or not. The documents may come from teaching and research institutions in France or abroad, or from public or private research centers.

L'archive ouverte pluridisciplinaire **HAL**, est destinée au dépôt et à la diffusion de documents scientifiques de niveau recherche, publiés ou non, émanant des établissements d'enseignement et de recherche français ou étrangers, des laboratoires publics ou privés.

1        **Seasonal and interannual variations of suspended particulate**  
2 **matter in a West-African lagoon (Nokoué lagoon, Benin): impact of**  
3 **rivers and wind**

4        **Indrig Laetitia NTANGYONG<sup>1,2, \*</sup>, Alexis CHAIGNEAU<sup>1,2,3</sup>, Yves MOREL<sup>3,4</sup>, Arnaud**  
5 **ASSOGBA<sup>2,5</sup>, Victor Olaègbè OKPEITCHA<sup>1,2,5,6</sup>, Thomas DUHAUT<sup>3</sup>, Thomas**  
6 **STIEGLITZ<sup>7</sup>, Pieter VAN BEEK<sup>3</sup>, Ezinvi BALOITCHA<sup>1</sup>, Zacharie SOHOU<sup>2,8</sup>, Vincentia**  
7 **M. C. HOUSSOU<sup>9</sup>, Sylvain OUILLON<sup>3,10</sup>**

8        1: International Chair in Mathematical Physics and Applications (ICMPA–UNESCO  
9 Chair)/University of Abomey-Calavi, Cotonou, Benin

10       2: Institut de Recherches Halieutiques et Océanologiques du Bénin (IRHOB), Cotonou, Benin

11       3: Laboratoire d'Études en Géophysique et Océanographie Spatiale (LEGOS), Université de  
12 Toulouse, CNES, CNRS, IRD, UPS, Toulouse, France

13       4: Laboratoire d'Océanographie Physique et Spatiale (LOPS), University of Brest, CNRS, IRD,  
14 Ifremer, IUEM, France

15       5: Institut de Recherche pour le Développement (IRD), Cotonou, Bénin

16       6: Laboratoire d'Hydrologie Appliquée (LHA), Institut National de l'Eau (INE), African  
17 Centre of Excellence for Water and Sanitation (C2EA), Université d'Abomey Calavi, Bénin

18       7: Aix Marseille Univ, CNRS, IRD, INRAE, CEREGE, Aix-en-Provence, France

19       8: Département de Zoologie, Faculté des Sciences et Techniques (FAST/UAC), Bénin

20 9: Laboratoire d'Etude et de surveillance Environnementales (LESE), Cotonou, Benin

21 10: Department of Water–Environment–Oceanography (WEO), University of Science and  
22 Technology of Hanoi (USTH), Vietnam Academy of Science and Technology (VAST), Hanoi,  
23 Vietnam

24 \*Corresponding author: ndjamoindrig@gmail.com

## 25 **Abstract**

26           This study, based on five years of monthly in situ data collected from 2018 to 2022,  
27 examines the seasonal and interannual fluctuations of suspended particulate matter (SPM)  
28 concentration in Nokoué Lagoon, Benin. Seasonally, SPM exhibits significant variations primarily  
29 influenced by changes in river discharge. During low-flow periods (December to May), SPM  
30 concentrations are relatively low ( $<15 \text{ mg L}^{-1}$ ) throughout the lagoon. During this time, slight  
31 temporal variations are correlated with wind energy and likely associated with wind-induced  
32 resuspension of sediments. This is confirmed by slightly higher concentrations of SPM in the  
33 bottom layers compared to the surface. Resuspension appears to be lower in the west than in the  
34 east, likely due to the increased presence of *acadjas* (brush parks) in the west, reducing fetch and  
35 wind intensity, thus decreasing resuspension. At the onset of the river flood period (July-August),  
36 associated with the West African monsoon, increased river flow generates a significant turbid  
37 plume extending from the northeast of the lagoon to the Cotonou channel, connecting the lagoon  
38 to the Atlantic Ocean. SPM levels then increase considerably ( $>100 \text{ mg L}^{-1}$ ), with a pronounced  
39 SPM gradient from the western to eastern regions of the lagoon. The less dense freshwater laden  
40 with sediment from the rivers flows over the denser saline water of the lagoon, leading to slightly  
41 higher SPM concentrations in the surface layers. Between September and November, SPM  
42 concentration gradually decreases as river flows reach their peak values. Thus, on a seasonal scale,  
43 the relationships between SPM and river discharge show a temporal lag, resulting in a clockwise  
44 hysteresis cycle. This is explained by the early mobilization of fine sediments during rising river  
45 flows, followed by reduced sediment availability and dilution effects as the flood peaks. On an  
46 interannual scale, SPM variations are relatively low with slight temporal shifts observed in the  
47 formation and expansion of the turbid plume and peak SPM levels. The total SPM mass in the

48 lagoon ranges from 0.2 to  $0.3 \times 10^4$  tonnes during low-flow periods to  $20\text{-}30 \times 10^4$  tonnes at the onset  
49 of flooding. We also discuss uncertainties associated with SPM determination, estimated at  
50 approximately 5-15%. This study leverages a unique database in West Africa and provides  
51 valuable insights into the hydro-sedimentary dynamics of Nokoué Lagoon.

52 **Keywords:** Suspended particulate matter; seasonal and interannual variability; lagoon; Nokoué;  
53 resuspension; sediments.

## 54 **1. Introduction**

55 Coastal lagoons, encompassing approximately 13% of the world's coastline (Barnes, 1980) are  
56 characterized by pronounced variations in their physical, biogeochemical, and biological  
57 parameters. Lagoons, acting as transitional zones between the land and the ocean, generally exhibit  
58 a dynamic behavior driven by the interplay of freshwater and saltwater exchanges. Being among  
59 the most productive ecosystems globally, they provide vital ecosystem services that cater to  
60 diverse activities such as aquaculture, fishing, recreation, tourism, sand extraction, and  
61 transportation (Macintosh, 1994; Alongi, 1998; Spurgeon, 1999 Pérez-Ruzafa et al., 2012). The  
62 effective management of these aquatic systems relies upon an in-depth understanding of their  
63 functioning.

64 The concentration of suspended particulate matter (SPM) in the water column is an important  
65 environmental parameter influencing the functioning of coastal lagoons. Spanning a size range  
66 from a few  $\mu\text{m}$  to several hundred  $\mu\text{m}$ , SPM exerts a significant influence on biogeochemical  
67 cycles and water quality through various processes. On one hand, both inorganic and organic SPM  
68 attenuate light, resulting in reduced photosynthesis and subsequent oxygen production, thereby  
69 impacting primary production and biological activity (Davies-Colley and Smith, 2001). On the

70 other hand, SPM also affects water quality by serving as sites for aggregation and adsorption of  
71 pollutants onto their surfaces (Etemad-Shahidi et al., 2010; Hossain et al., 2004). Consequently,  
72 these adsorbed pollutants can accumulate within the trophic chain, particularly through filter-  
73 feeding organisms, while also being transported and subsequently deposited as sediments in  
74 sediment reservoirs.

75 Transport and deposition of suspended particulate matter (SPM) play a critical role in  
76 facilitating sediment redistribution among watersheds, lagoon environments, and the marine  
77 ecosystem (Kari et al., 2017; Ouillon, 2018). The inherent variability in SPM inputs contributes to  
78 morphodynamic changes observed in diverse environments such as rivers, lagoons, barrier  
79 beaches, or deltas, thereby influencing flood control, irrigation, navigation, aquaculture and  
80 aquatic habitats (Poff et al., 1997; Barbier et al., 2011; Weston et al., 2014). Monitoring, analyzing,  
81 and understanding spatial and temporal variability of SPM is an important step towards a holistic  
82 quantification of sediment budgets in order to ensure the sustainable management of coastal and  
83 inland water ecosystems.

84 Variations in suspended particulate matter (SPM) concentrations within a lagoon's water  
85 column are influenced by a range of factors, encompassing internal and external forcings.  
86 Internally, these variations stem from phenomena such as shoreline runoff caused by rainfall or  
87 the resuspension of sediments due to wind-induced currents and waves. External influences are  
88 the transportation of particles eroded from the watershed, found in the riverbed and on its banks.  
89 Furthermore, oceanic factors, particularly tides, also contribute to SPM variations. Collectively,  
90 these diverse forcings contribute to the complex dynamics of SPM concentrations within a lagoon's  
91 water column.

92 Along West Africa, between Ivory Coast and Nigeria, the coastal zone comprises a series of  
93 lagoons (Allersma and Tilmans, 1993; Lalèyè et al., 2007; Adite and Winemiller, 1997; Adite et  
94 al., 2013). Among these lagoons, Nokoué lagoon, Benin's largest water body (covering ca. 150  
95 km<sup>2</sup>), is of significant ecological and socio-economic importance. Designated as a site of  
96 international importance under the Ramsar Convention on wetlands, this lagoon is regarded as one  
97 of West Africa's most biologically productive ecosystems, supplying 70% of Benin's continental  
98 fisheries (Lalèyè et al., 2007). It is flanked by three major urban centers (Cotonou, Abomey-Calavi,  
99 and Sémè Podji), with a combined population of over 1.5 million people. Moreover, it is home to  
100 West Africa's largest lakeside villages, accommodating 60,000 individuals living in stilt houses  
101 (Principaud, 1995), including approximately 15,000 fishermen. The local communities rely on this  
102 water body not only for fishing, capturing around 15,000 tonnes of fish annually (Principaud,  
103 1995), but also for domestic water supply, agriculture, market gardening, livestock breeding, etc.  
104 However, in addition to its inherent natural variability (e.g., Djihouessi and Aina, 2018; Chaigneau  
105 et al., 2022; 2023; Okpeitcha et al., 2022), Nokoué lagoon faces substantial challenges due to  
106 extensive anthropogenic pressures, resulting in declining water quality (Adjahouinou et al., 2012;  
107 2014; Aina et al., 2012a; 2012b), increasing eutrophication (Negusse and Bowen, 2010; Mama et  
108 al., 2011), and progressive sediment accumulation (Djihouessi et al., 2017).

109 Over the course of several decades, numerous studies have been conducted to elucidate the  
110 general hydro-ecological functioning of Nokoué lagoon (see Djihouessi and Aina, 2018 for a  
111 review). However, these investigations primarily rely on sporadic observations. Nevertheless, the  
112 global comprehension of sediment dynamics and SPM in the lagoon remains limited. Regarding  
113 sediment composition, more than two decades ago, the lagoon was predominantly characterized  
114 by silt (composed of very fine particles) in its western and southeastern regions, while its eastern

115 part consisted of sand (composed of fine and medium grains) (Gadel and Texier, 1986; Adounvo,  
116 2001). In the water column, based on five field campaigns conducted in 2015, Zandagba et al.  
117 (2016a) demonstrated that water turbidity and SPM concentrations were elevated in the eastern  
118 part of the lagoon, peaking in September during the flood season. Although this work provides  
119 preliminary insights into the nature of surface sediments and the variability of SPM in Nokoué  
120 lagoon, it is constrained in terms of temporal and spatial coverage, not allowing a full  
121 understanding of the underlying physical mechanisms driving the observed variability. Since the  
122 end of 2017, a multidisciplinary observational program has been implemented in Nokoué lagoon,  
123 enabling systematic and continuous data collection to enhance our understanding of this ecosystem  
124 (e.g., Chaigneau et al., 2022; Okpeitcha et al., 2022; Morel et al., 2022; Chaigneau et al., 2023).  
125 The objective of our study is to leverage this extensive database, comprising 60 monthly field  
126 campaigns, i) to describe the spatial distributions of sediments, SPM, and their organic (Particulate  
127 Organic Matter, POM) and inorganic (Particulate Inorganic Matter, PIM) fractions, and ii) to  
128 investigate the seasonal and interannual variations of SPM in the lagoon while elucidating the  
129 driving factors responsible for these observed fluctuations.

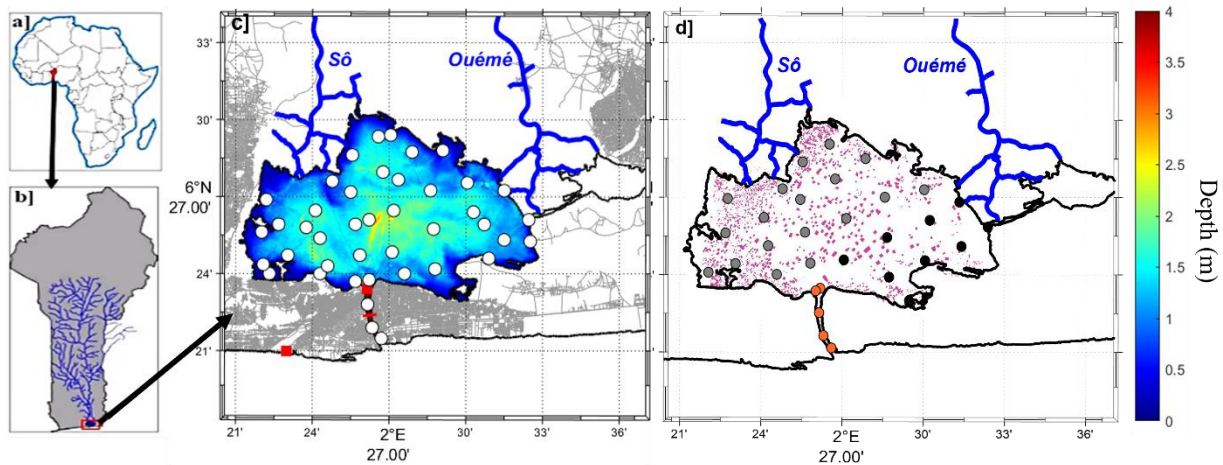
## 130 **2. Data and methods**

### 131 **2.1. Study area**

132 Nokoué lagoon, situated between 6°21'N and 6°30'N latitude and 2°21'E and 2°33'E longitude,  
133 has an average depth of 1.3 m and encompasses an approximate area of 150 km<sup>2</sup> at low flow  
134 (Chaigneau et al., 2022; Fig.1c). It stretches around 20 km from east to west and 11 km from south  
135 to north, and it is connected to the Atlantic Ocean through the Cotonou channel in its southern  
136 section (4.6 km long and 300 m wide), as well as to the Porto-Novo lagoon in its eastern part via



137 the Totchè channel (4.5 km long) (Fig. 1c). Along its northern shoreline, the two main rivers flow  
 138 into the lagoon: the Sô River, with a length of 85 km draining a small watershed of approximately  
 139 1000 km<sup>2</sup>, and the 500 km long Ouémé River draining a substantial watershed of roughly 50,000  
 140 km<sup>2</sup> to the north of the lagoon (Le Barbé et al., 1993; Djihouessi et al., 2017).



141

**Fig. 1:** Nokoué lagoon (Benin) and hydrographic stations investigated between January 2018 and December 2022. a) Location of Benin in West Africa. b) Hydrographic network of the Sô and Ouémé watersheds. c) Bathymetry of the lagoon during low-flow period (in color) together with the locations of the sediment samples collected to study the grain size and sediment composition and physical forcing stations. The white dots represent the 42 sediment sampling stations. The red squares represent the water level station south of the lagoon and the meteorological station at Cotonou airport. The ADCP section is depicted as a red line at the center of the Cotonou channel. d) Location of the 31 monthly SPM and CTD stations; stations shown in orange, black and gray represent the Cotonou channel, the eastern zone and the central/western zone of the lagoon, respectively (see Section III.3); The pink background map illustrates the distribution of acadjas identified by Chaffra et al. (2020).

142 The Ouémé watershed, which represents the primary freshwater and sediment source for  
 143 Nokoué lagoon lies in two distinct climatic zones. In the northern region, a tropical climate prevails  
 144 with a rainy season extending from May to October, peaking in August-September (Mama et al.,

145 2011; Djihouessi et al., 2017; Djihouessi and Aina, 2018). On the other hand, the southern Ouémé  
146 delta, where the river enters the lagoon, has a sub-equatorial climate characterized by two rainy  
147 seasons: a long rainy season from mid-March to mid-July and a short rainy season in September  
148 to October (Mama et al., 2011; Djihouessi et al., 2017; Djihouessi and Aina, 2018).

149 The average annual rainfall ranges from 960 mm in the northern part of the Ouémé basin to  
150 1340 mm in the southern part (Djihouessi et al., 2017). Under the influence of these hydrological  
151 patterns, Nokoué lagoon exhibits three distinct hydrological periods (Chaigneau et al., 2022;  
152 Okpeitcha et al., 2022; Morel et al., 2022): a flood period from September to November,  
153 characterized by a water level rise of approximately 90 cm and nearly zero salinity; a low-flow  
154 period from December to mid-May, during which the lagoon experiences minimal water levels  
155 and maximum salinity ( $S \sim 25$ ); and an intermediate period from June to August, where the water  
156 level slightly increases and salinity decreases due to heavy local rainfall in southern Benin (Texier  
157 et al., 1979; Le Barbé et al., 1993; Gnohossou, 2006).

158 The dynamics of Nokoué lagoon is further influenced by the prevailing monsoon winds, which  
159 result from the deflection of the equatorial trade winds (Eltahir and Gong, 1996). These dominant  
160 warm and humid winds blow consistently from the southwest throughout the year, with an average  
161 speed of  $3.5 \text{ m s}^{-1}$  (Colleuil and Texier, 1987). During December and January, the region  
162 experiences episodes of the Harmattan wind, a relatively cold and dry wind originating from the  
163 northeast. Both trade winds and Harmattan winds can have, through the generation of wind-  
164 induced currents or waves, a notable impact on sediment resuspension, consequently affecting the  
165 concentration of SPM in the Nokoué lagoon.

166 Nokoué lagoon features an abundance of artificial fishing parks called *acadjas*, made up of a  
167 substantial quantity of brushwood. *Acadjas* serve as sanctuaries and breeding grounds for aquatic  
168 species (Villanueva et al., 2006). According to *Chaffra et al. (2020)*, *acadjas* presently cover an  
169 area of 16.5 km<sup>2</sup>, representing approximately 16% of the lagoon's surface during the dry season,  
170 with a higher concentration in the western and northwestern parts of the lagoon (Figure 1d). The  
171 decomposition of organic matter from these *acadjas* can lead to oxygen depletion, causing the  
172 lagoon's waters to become less oxygenated, altering the composition of suspended solids and  
173 sediments, and potentially contributing to the lagoon's silting due to reduction in water flow in and  
174 around the *acadjas* (Niyonkuru and Lalèyè, 2010; Mama et al., 2011; Djihouessi et al., 2017).

## 175 **2.2. Turbidity and suspended particulate matter data**

176 Between January 2018 and December 2022, a total of 60 monthly campaigns, each lasting 2  
177 days, were conducted in the Nokoué lagoon. During each campaign, 31 vertical turbidity profiles  
178 were collected (Fig. 1d) using a Valeport MIDAS CTD+ 300 probe equipped with a turbidity  
179 sensor, with a vertical resolution of 0.1 dbar (~10 cm).

180 From April 2019 to December 2021, SPM concentrations were determined at each station  
181 following a commonly applied protocol (e.g., Neukermans et al., 2012; Moreina et al., 2013). At  
182 each station, a water sample was collected from the surface using a bucket for filtering. The volume  
183 of water filtered varied between 20 and 1000 ml depending on the turbidity level. Two types of  
184 filters were used for analysis: nuclepore polycarbonate (PC) membranes with a porosity of 0.4 µm  
185 for total SPM content, and GF/F glass fiber filters with a porosity of 0.7 µm to estimate the organic  
186 (POM) and inorganic (PIM) fractions of SPM. For each monthly campaign, the SPM data obtained  
187 from the 31 stations were spatially interpolated onto a regular grid with a resolution of

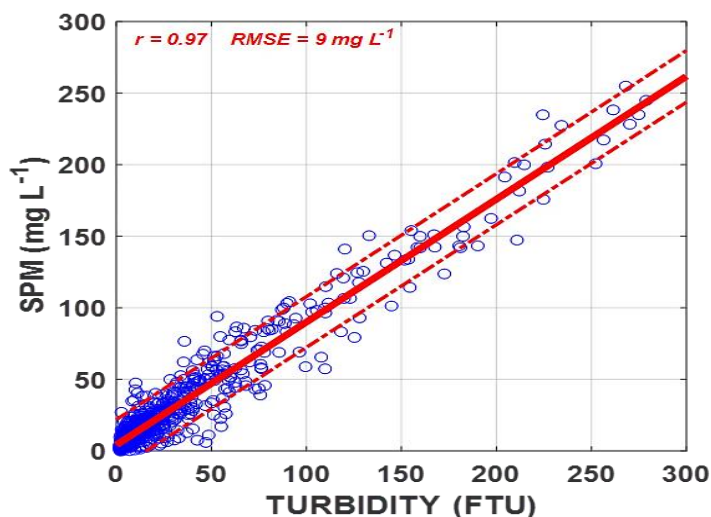
188 approximately 100 m × 100 m, using an objective interpolation scheme (Bretherton et al., 1976;  
189 McIntosh, 1990; Wong et al., 2003).

### 190 2.3. Determination of SPM from turbidity

191 Fig. 2 illustrates the relationship between surface turbidity and SPM distribution, based on 971  
192 pairs of observations gathered from April 2019 to December 2021. The distribution reveals a  
193 significant linear correlation ( $p < 0.001$ ) described by the following equation:

$$194 \text{ SPM} = 0.86 \times \text{Turbidity} + 4.3$$

195 where Turbidity is measured in FTU (Formazin Turbidity Units) and SPM in  $\text{mg L}^{-1}$ . This  
196 correlation exhibits a strong correlation coefficient ( $r = 0.97$ ) and a root mean square error (RMSE)  
197 of  $9 \text{ mg L}^{-1}$ . Consequently, this relationship enables the reconstruction of SPM levels in the lagoon  
198 using turbidity data collected by CTD over an extended period (2018-2022). This reconstruction  
199 facilitates the examination of seasonal and interannual variations in SPM within the lagoon.



200  
Fig. 2: Relationship between SPM (measured in situ) and turbidity (measured by an optical sensor), obtained from 971 pairs of measurements. The solid red line corresponds to the linear relationship, while the dashed lines delimit

*the 95% confidence interval. The correlation coefficient (r) and root mean square error (RMSE) are also provided in red.*

## 201 **2.4. Sedimentological data**

202 In February and April 2019, two campaigns were conducted to specifically determine the  
203 composition and grain size of sediment within the lagoon, covering a total of 42 stations (Fig. 1c).  
204 At each station, three surface sediment samples were extracted using an Ekman grab sampler.  
205 These samples were combined, thoroughly mixed, and a 500 g portion was retained for subsequent  
206 laboratory analysis. After drying the sediment at 60°C for 48 hours, the weight of the dry sediment  
207 was recorded, and the fine fraction was separated through wet sieving using a 45 µm mesh sieve.  
208 The remaining sediment (>45 µm) was then dried and weighed to determine the mass of the finest  
209 fraction (<45 µm) by calculating the difference in mass.

210 The sediment was further sieved using a vibrating column equipped with eight sieves (with  
211 mesh sizes of 4 mm, 2 mm, 1 mm, 500 µm, 250 µm, 125 µm, 63 µm, and 45 µm) for a duration  
212 of 15 minutes. The sediment retained on each sieve was weighed to determine the dry mass for  
213 each of the eight particle size classes. To determine the proportion of sediment in each particle size  
214 class at each station, the mass of each class was divided by the total dry mass. According to  
215 Wenworth's (1922) classification, three primary particle size classes were defined: very fine clays  
216 and silts below 45 µm, fine to coarse silts ranging between 45 µm and 63 µm, and very fine to fine  
217 sands ranging from 63 µm to 250 µm. The sediment fraction corresponding to these three classes  
218 was assessed at the 42 sampling stations and subsequently spatially interpolated using the same

219 objective interpolation scheme employed for the SPM and turbidity maps (Bretherton et al., 1976;  
220 McIntosh, 1990; Wong et al., 2003).

## 221 **2.5. River flow and wind speed**

222 To explore the drivers of the observed spatio-temporal variations in SPM concentration within  
223 the lagoon (as discussed in Section III), two key parameters were taken into consideration: (1)  
224 river flow, responsible for transporting SPM from catchments, and (2) wind, which generates  
225 waves and currents that can resuspend surface sediments in the water column through bottom shear  
226 stress (Maxam & Webber, 2010; Llebot et al., 2014; Jalil et al., 2019).

227 To obtain the time series of total river flows discharging into the lagoon for the period 2018-  
228 2022, water levels were continuously and frequently measured (every 20 minutes) at the mouth of  
229 the Cotonou channel and Nokoué Lagoon (Fig. 1c) using an immersed pressure sensor (Onset  
230 HOBO U20L-01; Chaigneau et al., 2022), and converted to water flow using a rating curve  
231 obtained from 33 pairs of simultaneous water level and flow measurements taken at different times  
232 of the year and covering all hydrological seasons (see Supplementary Material). The net tidally-  
233 averaged outflow from the Cotonou channel represent approximately the total river inflow entering  
234 the lagoon from the Sô et Ouémé watersheds (Supplementary Material; see also Morel et al.  
235 (2022)). It is important to note that rating curves can contain large errors, that can be due to several  
236 facts which are well describe in the supplementary material. In order to analyze the relationship  
237 between river inflow and SPM concentration, for each month between 2018 and 2022, the  
238 reconstructed flow rates are averaged over a 3-day period (prior and during data collection).

239 A wind time series, including direction and intensity at 10-m height was obtained from the  
240 National Meteorological Agency of Benin (METEO-BENIN: <https://meteobenin.bj/>) at Cotonou  
241 airport (red dot in Fig. 1c) at daily frequency for the study period of 2018-2022. Similar to flow

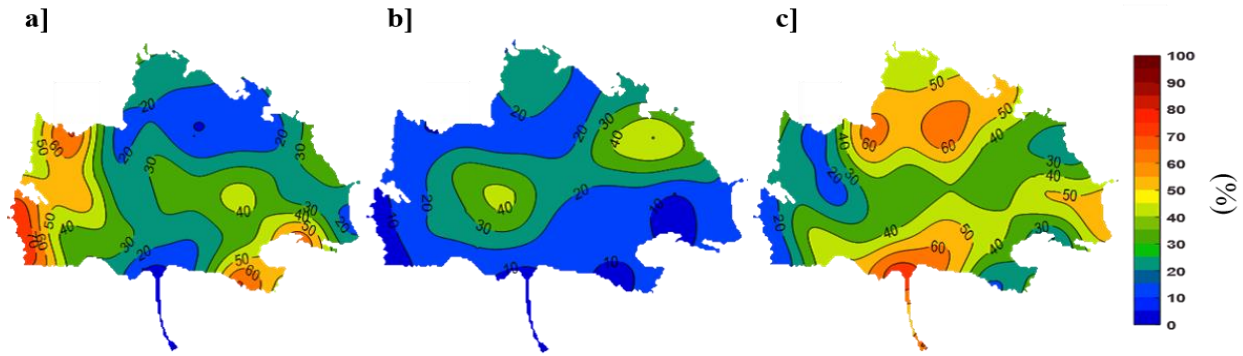
242 rates, these wind data were averaged over a 3-day period. Sensitivity tests were conducted,  
243 indicating that variations of this time window, ranging from 1 to 5 days prior to the campaign, had  
244 no significant impact on the obtained results. To investigate the potential influence of wind on  
245 sediment resuspension, the relationship between SPM and the square of wind intensity will be  
246 examined. This approach is employed because shear stresses at the bottom are directly proportional  
247 to wind stress, which in turn is proportional to the square of the wind intensity (Maxam & Webber,  
248 2010; Llebot et al., 2014; Jalil et al., 2018).

### 249 **3. Results**

#### 250 **3.1. Lagoon-scale characterization of sediments and suspended particulate** 251 **matter (SPM)**

##### 252 **3.1.1. Sediment distribution**

253 Fig. 3 shows the spatial distribution of sediments for the 3 particle size classes investigated  
254 (Section II.4). As mentioned in Section II.4, these data were collected during the 2019 low-flow  
255 period. Clay and very fine silts ( $<45\ \mu\text{m}$ ) are predominantly present in the western and southeastern  
256 zones (Fig. 3a); fine to coarse silts ( $45\text{-}63\ \mu\text{m}$ ) are mainly found in the northeast and center of the  
257 lagoon (Fig. 3b), while fine sands ( $63\text{-}250\ \mu\text{m}$ ) are dominant in the east and north, as well as  
258 around the Cotonou channel (Fig. 3c).



259

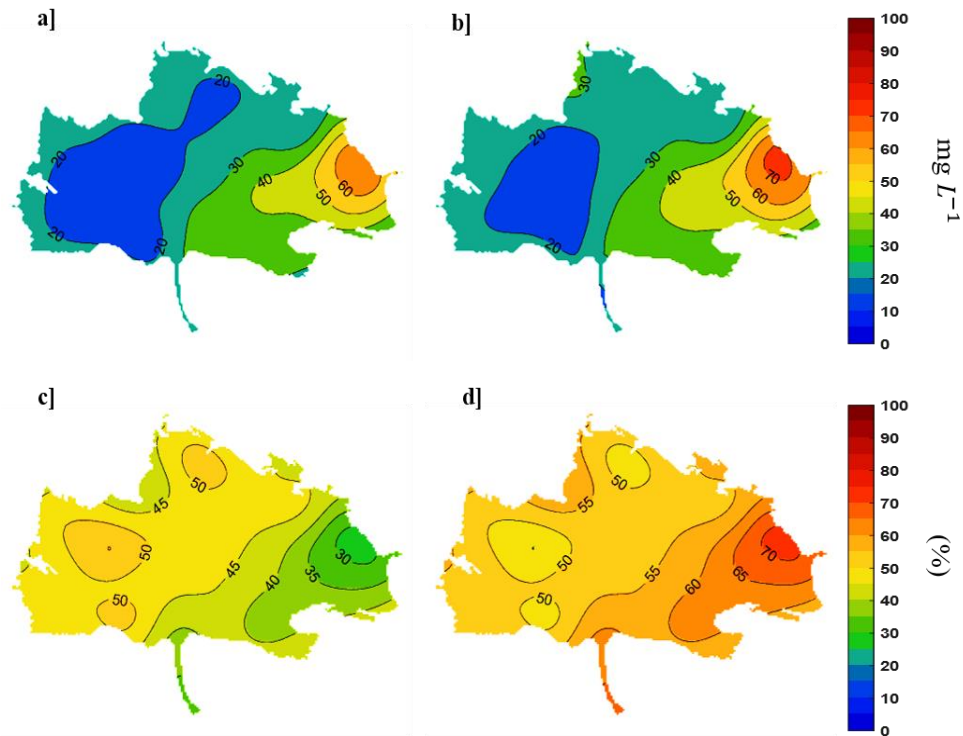
Fig. 3: Spatial distribution of sediment mass fraction (in %) for the 3 main particle size classes. a) clay and very fine silt (<45  $\mu\text{m}$ .) b) fine to coarse silts (45-63  $\mu\text{m}$ ). c) very fine to fine sands (63-250  $\mu\text{m}$ ).

### 260 3.1.2. Average suspended particulate matter distribution

261 SPM concentrations and the fractions of PIM and POM have notable spatial patterns in their  
 262 averaged distribution (average from April 2019 to December 2021) (Fig. 4). Surface and bottom  
 263 SPM concentrations exhibit significant variation, ranging from 12 to 75  $\text{mg L}^{-1}$ . The highest values  
 264 are observed in the eastern region, where a turbid plume extends between the mouth of the Ouémé  
 265 River and the Cotonou channel. Conversely, the lowest SPM values are found in the central and  
 266 western parts of the lagoon. The vertical differences in SPM concentration remain relatively small,  
 267 ranging from 0 to 10  $\text{mg L}^{-1}$  (Fig. 4a-b).

268 The average POM fraction shows strong variability, ranging from 25% to 60% (Fig. 4c). The  
 269 maximum values are observed in the western and northern areas, while the minimum values are  
 270 found between the eastern region and the Cotonou channel. Conversely, the PIM fraction exhibits  
 271 an inverse relationship to that of POM, reaching its maximum (~75%) towards the east, near the  
 272 mouth of the Ouémé River, and its minimum (<50%) in the western and northern regions (Fig.  
 273 4d).





274

Fig. 4: Average spatial distribution (April 2019-December 2021) of suspended solids (SPM in  $\text{mg L}^{-1}$ ) and organic (POM, in %) and inorganic (PIM, in %) fractions. a) SPM at surface. b) SPM at bottom. c) POM at surface. d) PIM at surface.

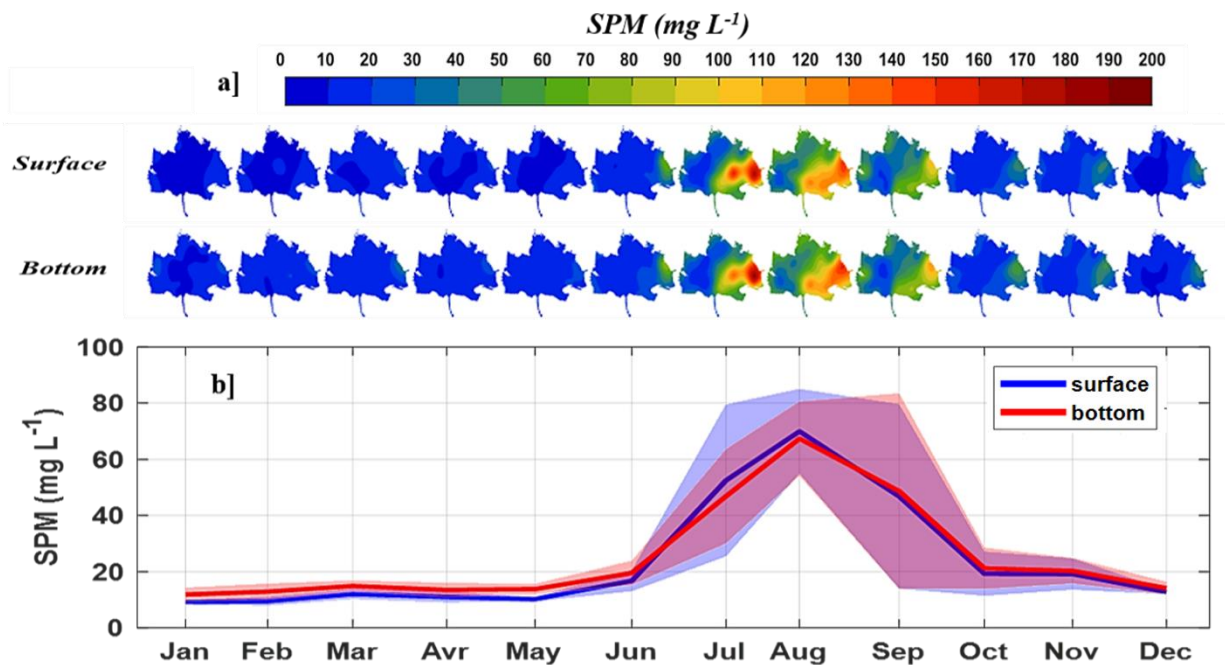
## 275 3.2. Seasonal and interannual variations in SPM

### 276 3.2.1. Seasonal variation

277 Fig. 5 illustrates the average seasonal variation in SPM concentrations observed between 2018  
 278 and 2022 and reconstructed from turbidity measurements. During the low-flow period from  
 279 January to May (Fig. 5a), the SPM concentration remains relatively low throughout the lagoon,  
 280 ranging from 5 to 30  $\text{mg L}^{-1}$ . In June, SPM concentration starts to increase at the Ouémé mouth,  
 281 and a turbid plume extending from the Ouémé to the Cotonou channel becomes visible between  
 282 July and September. During this period, relatively high SPM values (50-90  $\text{mg L}^{-1}$ ) are also  
 283 observed around the Sô area in the northwest of the lagoon. The maximum values are reached in

284 August, with an increasing gradient from west ( $30 \text{ mg L}^{-1}$ ) to east ( $200 \text{ mg L}^{-1}$ ). From October to  
 285 December, the SPM concentration significantly decreases ( $10\text{-}60 \text{ mg L}^{-1}$ ), reaching its minimum  
 286 in January (Fig. 5a).

287 Fig.5b depicts the monthly lagoon-averaged SPM concentrations, ranging from  $10 \text{ mg L}^{-1}$   
 288 during low-flow periods to  $70 \text{ mg L}^{-1}$  in August. The high standard deviations observed between  
 289 July and September indicate the pronounced spatial contrasts in SPM concentrations observed  
 290 during this period in Figure 5a. As further discussed in Section 4.1., during low-flow periods, the  
 291 mean SPM concentration at the bottom slightly exceeds that at the surface. However, in July and  
 292 August, the SPM concentrations at the surface are slightly higher than those at the bottom.

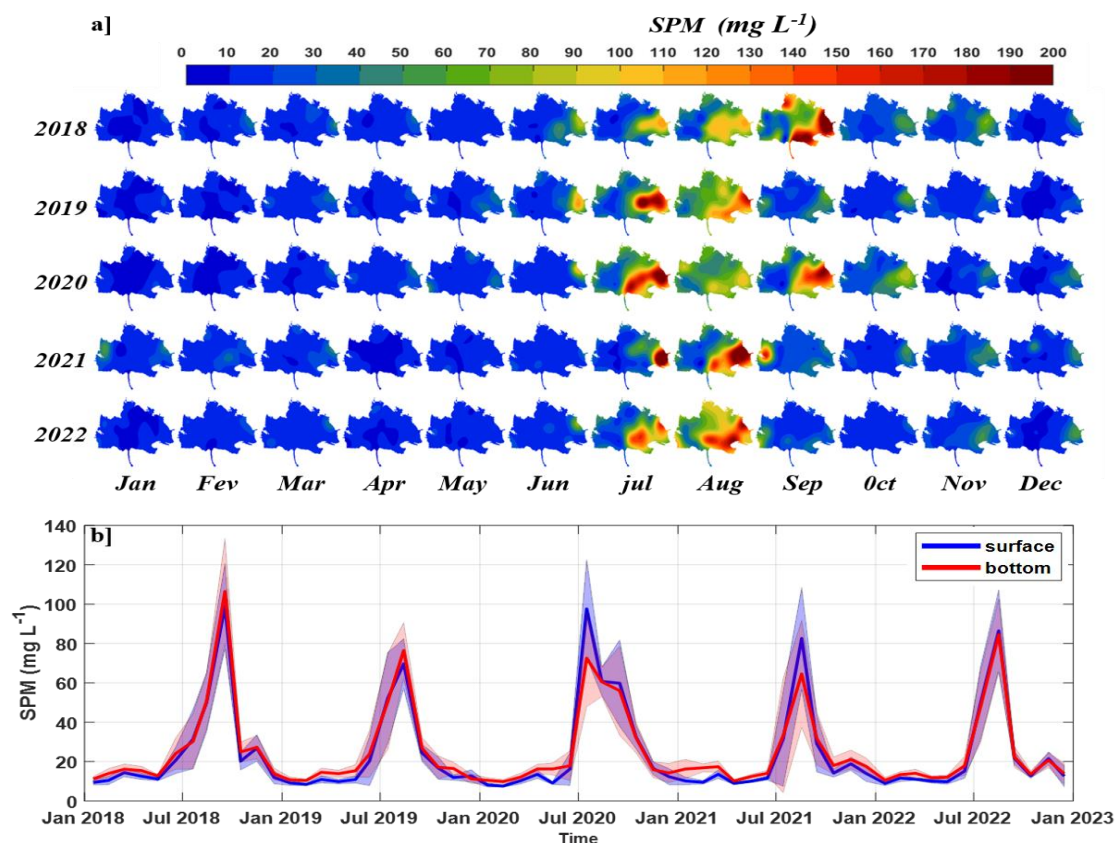


293 **Fig. 5:** Average seasonal cycle (2018-2022) of the SPM. a) Monthly spatial distribution at the surface (upper panel) and at the bottom (lower panel); climatological months are indicated at the bottom of b). b) Average monthly temporal evolution of the SPM in Nokoué lagoon.

294 **3.2.2. Interannual variation**

295 Interannual variations in surface SPM are shown on a monthly scale in Fig. 6a. The maximum  
296 SPM is systematically observed between July and september with some variability across the years  
297 resulting from interannual variations in river inflow. At the end of the flood period, the distribution  
298 and intensity of the Ouémé plume to the east differs from year to year: in December 2018 and  
299 2019, SPMs at the mouth of the Ouémé are much lower than in 2020-2022.

300 Fig. 6b shows that, on average in the lagoon, the SPM peak observed in July-August is higher  
301 in 2018 and 2022 (90-110 mg L<sup>-1</sup>) than in 2019-2021 (60-70 mg L<sup>-1</sup>). We also note that during the  
302 SPM peaks in 2020 and 2021, concentrations were higher at the surface.



303

Fig. 6: Monthly interannual variation in SPM. a) Monthly spatial surface distribution. b) Average monthly temporal evolution in Nokoué lagoon.

### 304 **3.3. Relationship between suspended matter and environmental drivers (river inflow and** 305 **wind speed)**

306 The spatial distributions of SPM and their temporal variability (Figs. 4 to 6) suggest that the  
307 study area can be divided into 3 sub-regions: the turbid plume zone in the east (black dots on Fig.  
308 1d), the zone of relatively low SPM concentration in the center and west (gray dots on Fig. 1d),  
309 and the Cotonou channel (red dots on Fig. 1d) corresponding to the lagoon outlet. It is important  
310 to note that a clustering analysis, which groups stations with similar SPM variations, was also  
311 conducted and yielded the same grouping (not shown). To determine the main drivers of SPM  
312 variability in the lagoon, we examined the temporal evolution of SPM in the 3 defined zones and  
313 their relationship with two key factors: river discharge and wind.

#### 314 **3.3.1. Impact of river inflow on SPM seasonal variability**

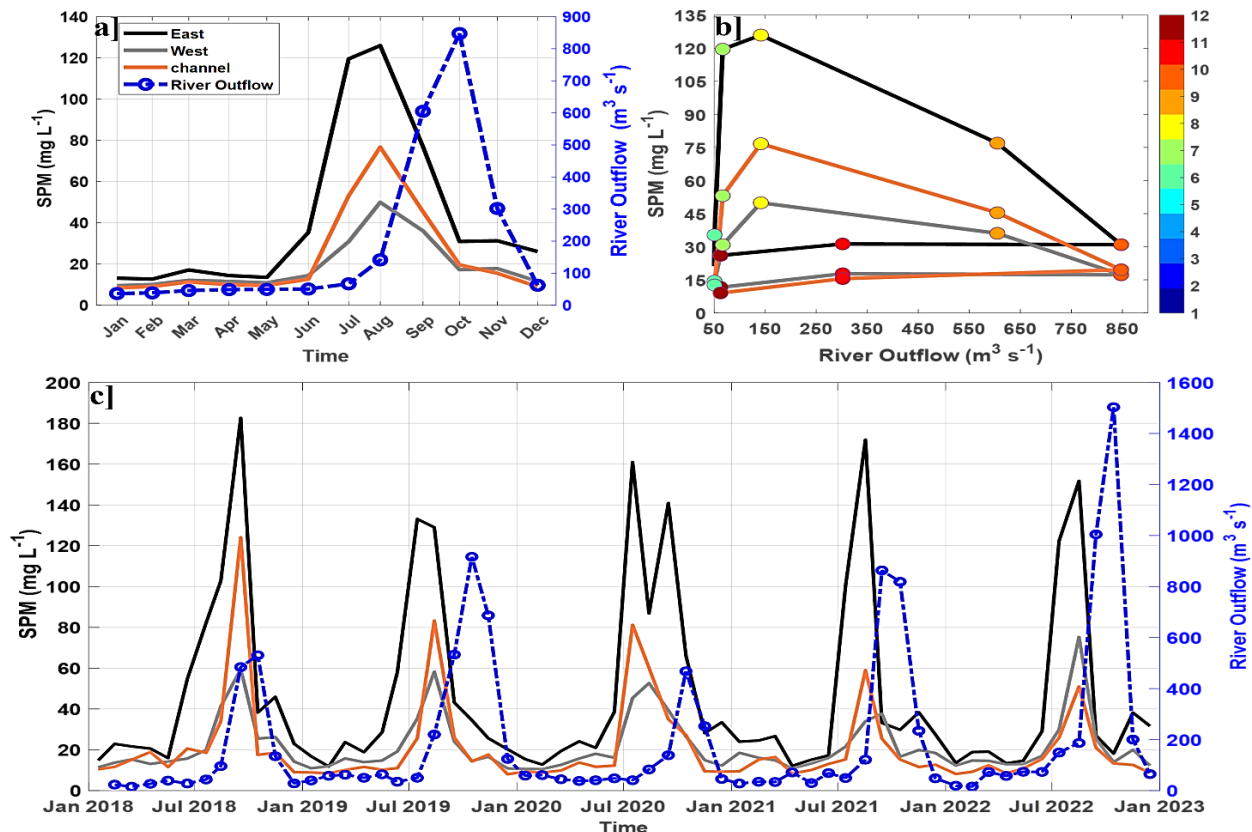
315 Fig. 7a presents the average seasonal cycle of SPM in the 3 predefined regions of the lagoon.  
316 In the eastern plume area, SPM concentrations reach an average of  $125 \text{ mg L}^{-1}$  in August, while in  
317 the western part of the lagoon, they are only  $50 \text{ mg L}^{-1}$  (Fig. 7a). The Cotonou channel exhibits an  
318 intermediate peak of  $80 \text{ mg L}^{-1}$ . From October to December, the eastern part of the lagoon has a  
319 higher sediment load ( $\sim 30 \text{ mg L}^{-1}$ ) than the western zone or the Cotonou channel ( $< 20 \text{ mg L}^{-1}$ ).  
320 Between January and May, the 3 zones show relatively similar SPM levels, ranging from 10 to 20  
321  $\text{mg L}^{-1}$ .

322 Comparing these variations with the seasonal cycle of river inflow (Fig. 7a) reveals four distinct  
323 phases. The first period, from January to May, corresponds to the low-water phase, during which  
324 both the SPM concentrations ( $< 20 \text{ mg L}^{-1}$ ) in the lagoon and the river flow ( $\sim 50 \text{ m}^3 \text{ s}^{-1}$ ) are low.  
325 The second phase, from June to August, coincides with the main rainy season in southern Benin

326 and the onset of the flooding period. During this period, river flows slightly increase (from 50 to  
327  $150 \text{ m}^3 \text{ s}^{-1}$ ), while SPM begin to rise in the east in June and subsequently increase sharply  
328 throughout the lagoon in July and August. The third phase, from August to October, represents the  
329 peak flooding phase, characterized by an average river flow of  $900 \text{ m}^3 \text{ s}^{-1}$ , while SPM levels  
330 decrease significantly ( $<40 \text{ mg L}^{-1}$ ). The last phase, in November and December, corresponds to  
331 the recession phase, with considerable reduction in flows and slight decline in SPM levels (around  
332  $10 \text{ mg L}^{-1}$ ). These relationships between SPM and river flow result in a clockwise hysteresis cycle  
333 (Fig. 7b), characterized by a SPM peak occurring prior to the peak of maximum flow (Fig. 7a). As  
334 further discussed in Section 4.1, the early mobilization of fine sediment during rising river flows,  
335 followed by reduced sediment availability and dilution effects as the flood peaks.

336 Fig. 7c illustrates the interannual variation in SPM in the 3 predefined regions of the lagoon.  
337 The eastern zone consistently exhibits higher SPM levels compared to the west and the Cotonou  
338 channel. The average maximum SPM values, observed at the head of the flood 1 to 3 months  
339 before maximum flows, range between  $130 \text{ mg L}^{-1}$  and  $180 \text{ mg L}^{-1}$  in the eastern zone, depending  
340 on the year. In the west, the values fluctuate between  $40 \text{ mg L}^{-1}$  and  $80 \text{ mg L}^{-1}$ , while in the Cotonou  
341 channel, they range between  $50 \text{ mg L}^{-1}$  and  $120 \text{ mg L}^{-1}$ . During the low-flow period, SPM  
342 concentrations display slight interannual variations of around  $10\text{-}25 \text{ mg L}^{-1}$  in the eastern zone and  
343  $5\text{-}15 \text{ mg L}^{-1}$  in the western zone and the Cotonou channel. Between 2019 and 2021, one-month lag  
344 can be observed in SPM peaks between zones, possibly attributed to the propagation time of the  
345 turbid plume from the East zone, where it forms, to the Central and Cotonou Channel zones, where  
346 it gradually expands (see also Fig. 6). Finally, a noteworthy observation is the occurrence of a  
347 double SPM peak exclusively in the east during July and September 2020, which does not coincide

348 with any distinct river flow pattern. Similarly, it is worth noting that the intensity of SPM peaks  
 349 does not show a direct temporal coincidence with the maximum intensity of river flows.



350  
 351  
 352  
 353  
 354  
 355  
 356

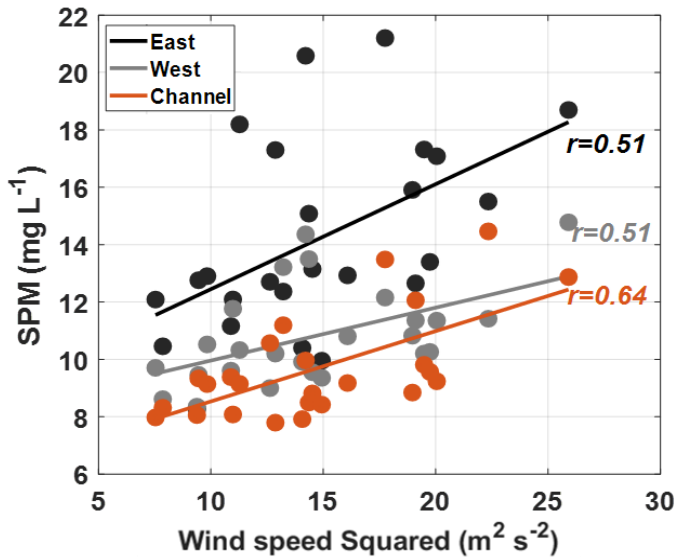
Fig. 7: Seasonal and interannual variations (2018-2022) in SPM and the sum of river discharges from the Sô and Ouémé rivers entering the lagoon. a) Average seasonal cycle (2018-2022) of SPM in the 3 sub-regions and discharges. b) Relationship between SPM and river discharges.

### 351 3.3.2. Impact of wind and sediment resuspension

352 Both wind energy and fetch, representing the uninterrupted distance over water that the  
 353 wind blows, play a crucial role in determining the size and energy of waves. Additionally, factors  
 354 such as the depth of water and sediment characteristics further modulate the intensity of sediment  
 355 resuspension. While the most significant seasonal fluctuations in SPM are primarily driven by  
 356 river inflow during high-flow periods, the relatively minor variations observed during low-flow

357 periods do not directly correspond to the hydrological regime of the rivers. We thus hypothesize  
358 that during this season (January to May) wind-induced processes may be responsible for the  
359 observed SPM variations through sediment resuspension.

360         The resuspension of sediment in the water column during low-flow period is also likely  
361 supported by Figures 5 and 6, showing a higher concentration of SPM in the bottom layer.  
362 Unfortunately, we lack current or wave data to thoroughly study the processes involved in the  
363 resuspension. However, Figure 8 reveals a notable finding: in all 3 sub-regions, a significant linear  
364 correlation can be observed between SPM concentrations during low-flow periods and the square  
365 of wind speed. The prevailing southwest winds are moderate, with values between 2.5 and 5.5 m  
366  $s^{-1}$ . The variations in wind speed squared and SPM exhibit a correlation of 50-65% during low-  
367 flow periods, with the strongest correlation being observed in the Cotonou channel. This suggests  
368 that wind-induced waves and currents likely contribute to the resuspension of sediment in the water  
369 column, thereby accounting for the observed fluctuations in SPM when river flows and water  
370 levels are low. Consequently, wind-driven resuspension emerges as a significant process  
371 contributing to SPM variability during this period. It is important to note that the amount of  
372 sediment resuspended by the wind is more pronounced but not significantly (greater linear slope  
373 in Fig. 8) in the eastern part of the lagoon compared to the western part, despite the sediments  
374 being coarser (refer to Fig. 3). As further discussed in Section 4, this is likely due to the higher  
375 concentration of *acadjas* in the western part of the lagoon (Figure 1d) that decrease the intensity  
376 of the wind-induced processes in the water column.



377

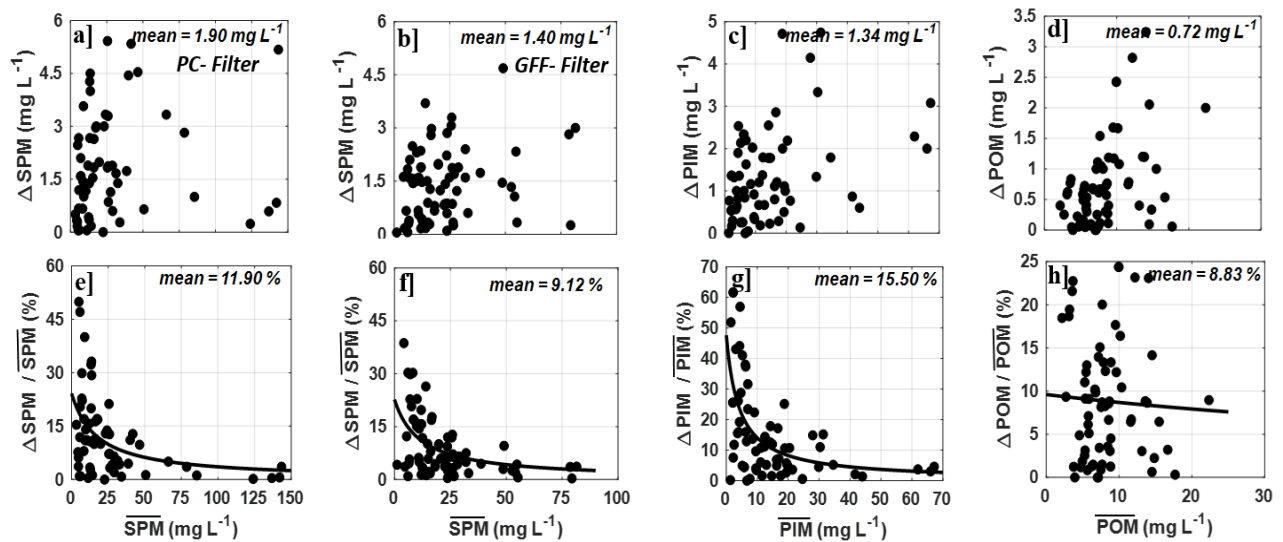
Fig. 8: Relationship between the mean SPM concentration in each sub-region and the squared wind speed during the low-flow months (January-May) of each year (2018-2022). For each of the 3 sub-regions, a linear fit is presented along with the corresponding correlation coefficient ( $r$ ). The colors black, gray and red correspond to the East, West and Cotonou Channel regions, respectively.

### 378 3.4. Uncertainties in SPM measurements

379 In order to quantify the uncertainties in SPM estimations, over 60 duplicate measurements of  
 380 SPM were conducted during campaigns carried out in different seasons and contrasting locations  
 381 within the lagoon, characterized by varying levels of turbidity. For each duplicate, the average  
 382 value of SPM from the 2 replicates ( $\overline{SPM}$ ) is calculated, as well as the absolute difference ( $\Delta SPM$ ,  
 383 en  $\text{mg L}^{-1}$ ) or relative difference ( $\Delta SPM / \overline{SPM}$ , en %). Similar analyses are performed for PIM and  
 384 POM. For all three variables (SPM, PIM et POM), the measurement differences between  
 385 duplicates do not significantly depend on concentration (Fig. 9a-d). Across all SPM duplicates, the  
 386 average difference is  $1\text{-}2 \text{ mg L}^{-1}$ , regardless of whether the measurements were obtained from



387 polycarbonate filters (Fig. 9a) or GF/F filters (Fig. 9b). Similarly, the uncertainties for PIM and  
 388 POM are  $0.7 \text{ mg L}^{-1}$  and  $1.3 \text{ mg L}^{-1}$ , respectively (Fig. 9c-d). The relative uncertainties (in %)  
 389 decrease as SPM concentrations increase (Fig. 9e-h) because, for a filtered water volume, there is  
 390 greater variability in the spatial distribution of particles in less turbid sampled waters (Doxaran et  
 391 al., 2012). On average, the uncertainties are approximately  $\sim 10\%$  for SPM (regardless of filter  
 392 type, Fig. 9e-f) and 15% and 9% for PIM (Fig. 9g) and POM (Fig. 9h), respectively. For SPM  
 393 ranges of 0-25, 25-50, and  $>50 \text{ mg L}^{-1}$ , the average relative uncertainty is 11%, 6%, and 2%,  
 394 respectively, for measurements obtained with GF/F filters, and 16%, 8%, and 2%, respectively,  
 395 for measurements obtained with polycarbonate filters. These values are consistent with the values  
 396 of 16%, 10%, and 2% obtained by Doxaran et al. (2012) for SPM concentrations ranging from  
 397 0.04–1, 1–10, and 10–100  $\text{mg L}^{-1}$ , respectively. Likewise, the relative uncertainties of POM and  
 398 PIM measurements decrease as the concentration increases.



399

Fig. 9: Distribution of measurement uncertainty as a function of their mean values. a-d] Absolute difference ( $\Delta\text{SPM}$ ,  $\Delta\text{PIM}$ ,  $\Delta\text{POM}$ , in  $\text{mg L}^{-1}$ ) of duplicates obtained on polycarbonate filters (a) and GF/F (b-d). e-h] Relative

difference (in %) of duplicates obtained on polycarbonate filters (e]) and GF/F (f-h]). Black curves represent best fits to the data.

## 400 **4. Discussion**

### 401 **4.1. Spatio-temporal variations of sediment and SPM**

402 The surface sediments in Nokoué lagoon are primarily composed of small particles, including  
403 clay, silt, and fine sand, as depicted in Figure 3. This spatial distribution closely resembles the  
404 findings reported more than three decades ago by Gadel and Texier (1986), suggesting that the  
405 hydrodynamic conditions and sediment composition in the lagoon have remained relatively stable  
406 over time. The finest particles are predominantly located in the western and southeastern regions  
407 of the lagoon, likely a result of reduced water circulation far from river mouths and Cotonou  
408 channel as well as the high density of *acadjas* (Niyonkuru and Lalèyè, 2010; Mama et al., 2011;  
409 Djihouessi et al., 2017; Chaffra et al., 2020). These *acadjas* impede current velocity and mitigate  
410 the resuspension of particles by wind, thereby facilitating their retention and accumulation. In  
411 addition, these areas are adjacent to major urban centers and receive a significant inflow of runoff  
412 from open storm drains (Afouda et al., 2004; Hountondji et al., 2019), which can transport fine  
413 particles into the lagoon. In the western part of the lagoon, an elevated concentration of POM was  
414 observed, consistent with Texier et al. (1979). This increase can be attributed to several factors.  
415 The greater presence of *acadjas* (Fig. 1d and Chaffra et al. (2020)), along with the decomposition  
416 of aquatic vegetation, leads to the production of organic-rich particles and the deposition of peaty  
417 sediments (Gadel and Texier, 1986). Indeed, the western zone of the lagoon is known for its  
418 significant seasonal influx and rapid proliferation of water hyacinths, which become trapped in the  
419 *acadjas* (Mama, 2010; Mama et al., 2011; Dovonou et al., 2011; Chaffra et al., 2020). As water

420 levels recede and salinity increases, these hyacinths naturally decay and decompose, resulting in  
421 the enrichment of organic matter within the water column. Moreover, recent research by  
422 Chaigneau et al. (2023) has emphasized the western zone of the lagoon as a favorable environment  
423 for abundant zooplankton, which may also contribute to the observed increase in POM.

424 In contrast, sediments near the mouths of the rivers Sô and Ouémé and Cotonou channel are  
425 dominated by fine sands. This can be attributed to the intensified currents resulting from fluvial  
426 and tidal inputs, which effectively transport and disperse the finer particles from the seafloor.  
427 Towards the eastern region of the lagoon, the Ouémé River inflow contributes significantly to the  
428 generation of a turbid plume, extending as far as the Cotonou channel during flood periods. The  
429 sediment input and influence of the Ouémé River on SPM levels exceed that of the Sô River,  
430 presumably due to the Ouémé's drainage area being fifty times larger. Consequently, a gradient in  
431 average SPM concentration between the western and eastern sections of the lagoon is observed,  
432 consistent with previous studies on water transparency in the lagoon (Adite and Winemiller, 1997;  
433 Mama, 2010; Zandagba et al., 2016a; Djihouessi and Aina, 2018). Regarding vertical variations,  
434 SPM levels exhibit little difference between surface and bottom due to the shallow depth of the  
435 lagoon, which justified the use of surface SPM only.

436 On a seasonal scale, our observations reveal a prominent peak in Suspended Particulate Matter  
437 (SPM) concentrations at the onset of the flood (Fig. 7), preceding the maximum discharge. This  
438 phenomenon is characterized by a clockwise hysteresis loop in the relationship between SPM and  
439 river discharge (Fig. 7b). This pattern has also been documented for decades in other lagoons or  
440 aquatic environments (Arnbord et al., 1967; Walling & Webb, 1981; Van Sickle & Beschta, 1983;  
441 Williams, 1989; Zăvoianu, 1996; Bhutiyani, 2000; De Sutter & Verhoeven, 2001; Picouet et al.,  
442 2001; Kumar et al., 2002; Banasik et al., 2005; Baca, 2008). According to these authors, during

443 early heavy rainfall events and the onset of river flow, fine particles are mobilized from the  
444 riverbanks, leading to the resuspension and transport of fine particles that had settled and  
445 accumulated on the watershed bed during the previous low-water and recession season. This fine  
446 sediment rests loosely on the riverbed and is easily eroded as flows increase. Consequently, a  
447 substantial influx of SPM into the Nokoué lagoon occurs at the onset of the flood, resulting in the  
448 formation and propagation of a turbid plume between the Ouémé and Cotonou channel. After the  
449 onset of the flood, the riverbed is covered with less easily entrainable sediments before the water  
450 discharge reaches its maximum, as observed elsewhere (Arnbord et al., 1967; Walling, 1974;  
451 Wood, 1977; VanSichle and Bechta, 1983; Williams, 1989). Indeed, according to Williams (1989),  
452 early depletion or flushing of fine sediments can occur due to a limited available supply or a  
453 sustained and/or very intense flood. Therefore, as the flood reaches its peak (September-  
454 November), the availability of fine sediments decreases in the Sô and Ouémé, leading to a  
455 reduction in SPM concentrations. Additionally, a second process can be invoked: during the flood,  
456 the lagoon level rises by approximately 0.9 meters (Chaigneau et al., 2022), corresponding to a  
457 70% increase in volume. Thus, assuming a constant sediment load, suspended solids dilute within  
458 a larger water volume, resulting in a decrease in their concentration during the flood.

459 During periods of low river flow, the observed variations in SPM cannot be solely attributed to  
460 flow conditions. Instead, wind-induced sediment resuspension emerges as a probable influencing  
461 factor (Fig. 8), aligning with findings from other expansive lagoons like Patos (Brazil) and Chilika  
462 (India), where wind drives SPM variations during relatively low river flows (Castelao and Moller,  
463 2003; Kumar et al., 2016). In shallow aquatic environments, sediment resuspension is strongly  
464 influenced by wind (e.g., Jalil et al., 2019; Maxam and Weber, 2010; Llebot et al., 2014) as it  
465 generates currents and waves interacting with the bottom layer. The resuspension of sediments and

466 nutrients by these mechanisms is well-documented (Luettich et al., 1990; Bengtsson & Hellström,  
467 1992; Arfi et al., 1993; Qin et al., 2000; Zhu et al., 2005). However, due to the absence of wave or  
468 current measurement data in Nokoué Lagoon, we are unable to analyze in detail the specific  
469 physical mechanisms responsible for the observed SPM variations, despite a relatively strong  
470 correlation between SPM concentration and wind energy. Nevertheless, we have noted that larger  
471 quantities of SPM are resuspended by the wind in the eastern zone compared to the western zone,  
472 where sediment particles are smaller in size and weight. This discrepancy is likely attributed to the  
473 prevalence of *acadjas* in the western zone, characterized by dense branches extending from the  
474 lagoon bottom up to 1-2 meters above the water surface during low-flow periods. These *acadjas*  
475 reduce both wind intensity and fetch at the water surface, thereby diminishing wind-induced  
476 currents, waves, and turbulence in that area. While we have emphasized the significant role of  
477 wind-induced resuspension in modulating SPM concentration during low-flow periods, future  
478 studies should specifically target different processes (currents, waves, turbulence). Achieving this  
479 requires deploying dedicated observation platforms (anemometers, wave gauges, current meters,  
480 etc.) at various locations within the lagoon, as well as inside and outside the *acadjas*, to assess  
481 their specific effects. This approach will contribute to confirming the results and processes  
482 discussed herein.

483 Generally, tidally-driven currents may play a role in the supply and resuspension of SPM, but  
484 the tidal amplitude in Nokoué lagoon is less than 5 cm (Chaigneau et al., 2022), and tidal currents  
485 are in the order of a few centimeters per second (Zandagba et al., 2016b). Therefore, their impact  
486 on SPM is expected to be minor compared to other driving forces, except perhaps in the Cotonou  
487 Channel where tidal currents are stronger (approximately  $0.5-1.5 \text{ m s}^{-1}$ ) (Zandagba et al., 2016b).

488 Based on our dataset, the relationship between tidal coefficients and SPM concentrations did not  
489 reveal any significant dependence in either the Nokoué lagoon or the Cotonou Channel.

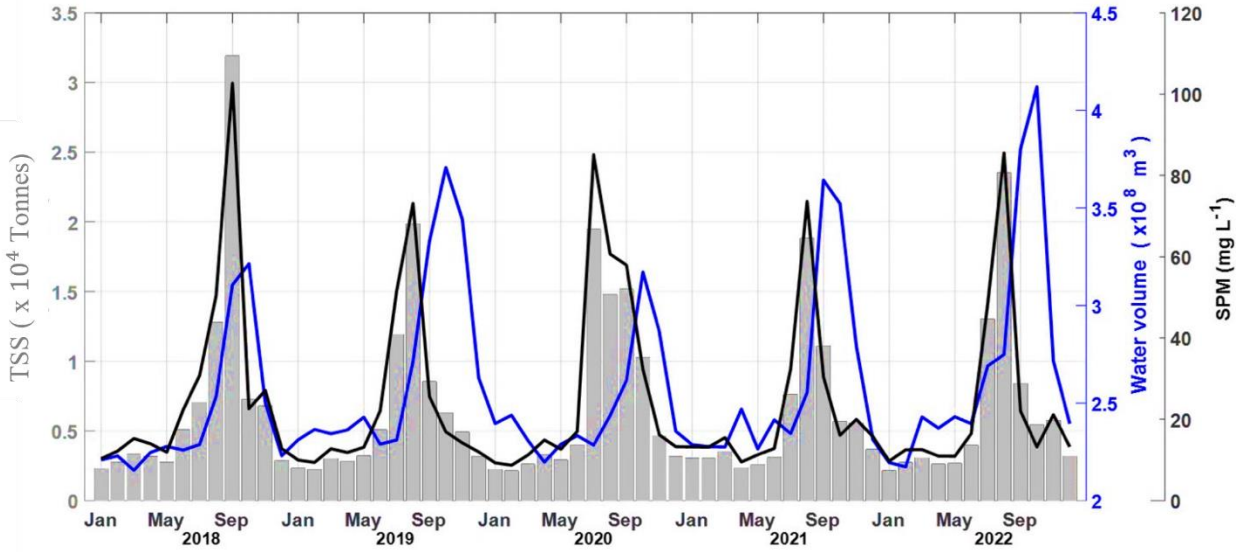
490 On the vertical, during periods of low water flow (January-May), the average SPM  
491 concentration at the lagoon bottom slightly exceeds that at the surface (Fig. 5 and 6), likely due to  
492 sediment resuspension leading to an increase in SPM-laden content in the bottom layer. However,  
493 in July and August, when SPM concentrations peak, the surface SPM levels slightly surpass those  
494 at the bottom. This can be attributed to the less dense SPM-laden freshwater from rivers, causing  
495 a 1-2 PSU increase from surface to bottom and resulting in lagoon stratification (Okpeitcha et al.,  
496 2022). As a consequence, a more laden turbid plume is observed at the surface, while the bottom  
497 layer is less laden. Such stratification is a characteristic of hypopycnal flow, which is commonly  
498 observed in lagoon systems connected to the open sea, as opposed to enclosed lakes where the  
499 opposite occurs and it is called hyperpycnal flow (Halfman & Scholz., 1993; Parsons et al., 2001;  
500 Mulder et al., 2003; Boggs, 2012; Zavala, 2020).

## 501 **4.2. Variation in total suspended solids in Nokoué lagoon**

502 Finally, we estimated the total amount of suspended solids (TSS, in tonnes) in the lagoon for  
503 each month of the study period (2018-2022). To do this, we used the entire set of turbidity profiles  
504 and the linear relationship established between SPM and turbidity (Section II.3) to reconstruct a  
505 three-dimensional SPM field. The TSS was then obtained by integrating the SPM field over the  
506 varying volume of the lagoon. It is important to note that the surface area of the lagoon during  
507 low-flow periods is 150 km<sup>2</sup> (Chaigneau et al., 2022), and its volume varies proportionally with  
508 the measured water levels.

509 The variability of TSS aligns qualitatively with that of the average SPM (Fig. 10). Specifically,  
510 there is a tenfold difference between minimum and maximum SPM, whereas the variation in  
511 volume is not even twofold. Consequently, when these factors are multiplied, TSS tends to be  
512 dominated (and thus exhibits phase coherence) by SPM variations rather than volume variations.  
513 However, this relationship is not strictly proportional to SPM due to the significant fluctuations in  
514 the lagoon's volume. Peaks in TSS within the lagoon coincide with periods of elevated water  
515 volume and high concentrations of suspended particles (SPM), whereas TSS reaches a minimum  
516 when both factors are at their lowest.

517 Large and highly variable quantities of suspended solids transit through the Nokoué lagoon,  
518 ranging from approximately 2000 tonnes to 32000 tonnes depending on the hydrological seasons,  
519 with an average value of around 6500 tonnes over the study period. Part of this total SPM load is  
520 contributed by rivers, while another part is associated with local sediment resuspension.  
521 Additionally, a portion is exported to the Atlantic Ocean through the Cotonou channel, while  
522 another portion settles and contributes to the infilling of the lagoon. These figures provide an initial  
523 estimation of the total SPM load in the Nokoué lagoon, but further measurements and studies are  
524 necessary to conduct a comprehensive sediment budget analysis of the lagoon. This budget will  
525 involve determining: i) the sediment input into the lagoon from the two main watersheds (Sô and  
526 Ouémé), ii) the export of sediments to the ocean through the Cotonou channel, and iii) the amount  
527 of sediment deposition in the Nokoué lagoon.



528

Fig. 10: Monthly variation of the total amount of suspended solids (TSS, gray vertical bars), water volume (blue line), and average concentration of SPM in the Nokoué lagoon from 2018 to 2022.

529 **5. Conclusion**

530 This study provides a thorough analysis of five years (2018-2022) of monthly SPM data in  
 531 Nokoué lagoon, Benin, aiming to characterize SPM variations and identify driving mechanisms.  
 532 SPM concentrations consistently remained below  $200 \text{ mg L}^{-1}$ . The SPM and river flow relationship  
 533 revealed a pronounced clockwise hysteresis cycle, with maximum SPM during the flood's onset  
 534 generating a turbid plume in the eastern zone. Low-flow periods (December-May) exhibited  
 535 minimum SPM levels, influenced by wind-induced resuspension. Interannually, SPM variations  
 536 were relatively low, with temporal shifts in turbid plume formation and peak SPM levels. The  
 537 study unveils sediment characteristics, highlighting differences between the western and eastern  
 538 zones.

539 These results provide a base for future research on different time scales not covered in this  
 540 study. For instance, it would be valuable to investigate the impact of flash floods on SPM inputs



541 to the lagoon at high frequencies, or the influence of African monsoon-induced wind gusts on  
542 sediment resuspension. Similarly, conducting a sediment balance in the lagoon at lower  
543 frequencies is crucial, which would involve quantifying the material input from the Sô and Ouémé  
544 catchments and determining the fraction exported to the Atlantic Ocean through the Cotonou  
545 channel. Estimating the rate of sedimentation and infilling of this shallow lagoon will require  
546 methods such as dating of sediment cores using natural and artificial radionuclides and numerical  
547 modeling. The obtained results offer important metrics and diagnostics for the development and  
548 calibration of a hydrosedimentary model, which could be used for scientific and management  
549 purposes.

550

## 551 **Acknowledgements**

552 Field surveys and instrumentation were supported by IRD and LEGOS. I. L. NTANGYONG  
553 was funded through a scholarship grant of the Deutscher Akademischer Austauschdienst (DAAD)  
554 in collaboration with the International Chair in Mathematical Physics and Applications (ICMPA–  
555 UNESCO Chair)/University of Abomey-Calavi (UAC), Cotonou, Benin. This work is a contribu-  
556 tion to the « JEA1 SAFUME » project funded by IRD and to the "Lagune Nokoué" TOSCA project  
557 funded by the French National Center for Space Studies (CNES). Special thanks to the members  
558 and crew participating to the bimonthly surveys, and in particular J. AZANKPO and P. AL-  
559 LAMEL.

560 **References**

561

562 Adite, A., Winemiller, K.O., 1997. Écologie trophique et écomorphologie des assemblages de  
563 poissons dans les lacs côtiers du Bénin, Afrique de l'Ouest. *Écoscience* 4 (1), 6-23.

564 Adite, A., Imorou, I., Gbankoto, A., 2013. Assemblages de poissons dans les écosystèmes de  
565 mangrove dégradés de la zone côtière, Bénin, Afrique de l'Ouest : Implications pour la  
566 restauration des écosystèmes et la conservation des ressources. *Journal of Environmental*  
567 *Protection* 4 (12), 1461-1475.

568 Adjahouinou, D., Liady, N., Fiogbe, E., 2012. Diversité phytoplanctonique et niveau de pollution  
569 des eaux du collecteur de Dantokpa (Cotonou-Bénin), *Int. J. Biol. Chem. Sci.* 6 (5), 1938-1949.

570 Adjahouinou, D.C., Yehouenou, B., Liady, M.N., Fiogbe, E.D., 2014. Caractérisation  
571 bactériologique des eaux résiduaires brutes de la ville de Cotonou (Bénin). *Journal of Applied*  
572 *Biosciences*, 78, 6705-6713.

573 Adounvo, D.U., 2001. Etude comparée de la productivité primaire des lacs Nokoué et Ahémé au  
574 Bénin. Thèse d'ingénieur Agronome, *Université Nationale du Benin*, Benin.

575 Afouda, A., Amani, A., Niasse, M., 2004. Réduire la vulnérabilité de l'Afrique de l'Ouest aux  
576 impacts du climat sur les ressources en eau, les zones humides et la désertification : éléments  
577 de stratégie régionale de préparation et d'adaptation, *IUCN*, Régional Office for Western Africa.

578 Aina, M., Degila, H., Chikou, A., Adjahatode, F., Matejka, G., 2012a. Risque d'intoxication par  
579 les métaux lourds (Pb, Cd, Cu, Hg) lié à la consommation de certaines espèces halieutiques  
580 dans le lac Nokoué : cas des crevettes de *Penaus* et du *Sarotherodon Melanotheron*. *British*  
581 *Journal of Science* 5 (1), 104-118.

582 Aina, M., Djihouessi, B., Vissin, E., Kpondjo, N., Gbèdo, V., Sohounhloué K., 2012b.  
583 Caractérisation des eaux usées domestiques et dimensionnalité d'une station pilote de traitement  
584 par lagunage à Abomey Calavi ville-Bénin. *J. Ingénierie Sci.* 1 (1), 45-50.

585 Allersma, E., Tilmans, W., 1993. Conditions côtières en Afrique de l'Ouest : un examen. *Gestion*  
586 *des océans et des côtes* 19, 199-240.

587 Alongi, D.M., 1998. Coastal Ecosystem Processes. Boca Raton: CRC Press.

588 Arfi, R., Guiral, D., Bouvy, M., 1993. Wind induced resuspension in a shallow tropical lagoon.  
589 *Estuarine, Coastal and Shelf Science*, 36(6), 587–604.

590 Baca, P., 2008. Hysteresis effect in suspended sediment concentration in the Rybárik basin,  
591 Slovakia / Effet d'hystérèse dans la concentration des sédiments en suspension dans le bassin  
592 versant de Rybárik (Slovaquie), *Hydrological Sciences Journal*, 53 :1, 224-235,

593 Banasik, K., Medeyski, M., Mitchell, J.K., Mori, K., 2005. An investigation of lag times for  
594 rainfall–runoff–sediment yield events in a small river basin, *Hydrol. Sci. J.* 50(5), 857–866.

595 Barbier, E.B., Hacker, S.D., Kennedy, C., Koch, E.W., Stier, A.C., Silliman, B.R., 2011. The  
596 value of estuarine and coastal ecosystem services. *Ecological monographs*, 81(2), 169-193.

597 Barnes, R.S.K., 1980. Coastal Lagoons: The Natural History of a Neglected Habitat, Vol. 106.  
598 *Cambridge University Press*, Cambridge.

599 Bengtsson, L., Hellström, T., 1992. Wind-induced resuspension in a small shallow lake.  
600 *Hydrobiologia*, 241(3), 163–172

601 Bhutiyani, M.R., 2000. Sediment load characteristics of a proglacial stream Siachen Glacier and  
602 the erosion rate in Nubra valley in Karakoram Himalayas, India. *J. Hydrol.* 227, 84–92.

603 Bretherton, F.P., Davis, R.E., Fandry, C.B., 1976. Une technique d'analyse objective et  
604 conception d'expériences océanographiques appliquées au MODE-73. *Profond. Rés. Océanogr.*  
605 *Abstr.*559-582.

606 Boggs, Sam., 2012. Principles of sedimentology and stratigraphy. Upper Saddle River, N.J.:  
607 Pearson Prentice Hall

608 Castelao, R.M., and Moller, O.O., 2003. Sobre a circulação tridimensional forçada por ventos na  
609 Lagoa dos Patos, Atlantica, 25, pp. 91–106.

610 Chaffra, A.S., Agbon, A.C., Tchibozo, E.A., 2020. Cartographie par télédétection des Acadjas,  
611 une technique de pêche illicite sur le lac Nokoué au Bénin. *Sci. Tech*, 5, 11-29.

612 Chaigneau, A., Okpeitcha, O.V., Morel, Y., Stieglitz, T., Assogba, A., Benoist, M., Sohou, Z.,  
613 2022. From seasonal flood pulse to seiche: multi-frequency water-level fluctuations in a large  
614 shallow tropical lagoon (Nokoué Lagoon, Benin). *Estuarine, Coastal and Shelf Science*, 267,  
615 107767.

616 Chaigneau, A., Ouinsou, F.T., Akodogbo, H.H., Dobigny, G., Avocegan, T.T., Dossou-Sognon,  
617 F.U., Azémar, F., 2023. Physicochemical drivers of zooplankton seasonal variability in a West  
618 African Lagoon (Nokoué Lagoon, Benin). *Journal of Marine Science and Engineering*, 11(3),  
619 556.

620 Colleuil, B., Texier, H., 1987. Le complexe lagunaire du lac Nokoué et de la lagune de Porto-  
621 Novo. In : Zones humides et lacs peu profonds d'Afrique. Chap. 3.- Répertoire UICN-WWF ;  
622 Ml. Burgis et J.J. Symoens (Publ.) - Coll. Travaux et Documents de l'Orstom, n° 211, pp. 188–  
623 196.

624 Davies-Colley, J., Smith, D., 2001. Turbidity, Suspended Sediment and Water Clarity: A Review.  
625 *Journal of the American Water Resources Association*, 37 (5), 1085–1101.

626 De Sutter, R., Verhoeven, R., 2001. Simulation of sediment transport during flood events:  
627 laboratory work and fields experiments. *Hydrol. Sci. J.*, 46(4), 599–610.

628 Djihouessi, M., Aina, M., Kpanou, B., Kpondjo, N., 2017. Mesure de la valeur économique totale  
629 du dragage de sable traditionnel dans le Complexe lagunaire côtier de Grand-Nokoué (Bénin).  
630 *Journal de la protection de l'environnement*, 8, 1605-1621.

631 Djihouessi, M.B., Aina, M.P., 2018. A review of hydrodynamics and water quality of Lake  
632 Nokoué: current state of knowledge and prospects for further research. *Reg. Stud. Mar. Sci.* 18,  
633 57–67.

634 Doxaran, D., Ehn, J., Bélanger, S., Matsuoka, A., Hooker, S., Babin, M., 2012. Optical  
635 characterisation of suspended particles in the Mackenzie River plume (Canadian Arctic Ocean)  
636 and implications for ocean colour remote sensing, *Biogeosciences*, 9, 3213–3229.

637 Dovonou, F., Aina, M., Boukari, M., Alassane, A., 2011. Physicochemical and bacteriological  
638 pollution of an aquatic ecosystem and its ecotoxicological risks: the case of Lake Nokoué in  
639 South Benin. *International Journal of Biological and Chemical Sciences*, 5(4), 1590-1602.

640 Eltahir, E.A.B., Gong, C., 1996. Dynamics of wet and dry years in West Africa. *Journal of*  
641 *Climate* 9: 1030–1042.

642 Etemad-Shahidi, A., Shahkolahi, A., Liu, C., 2010. Modeling of hydrodynamics and  
643 cohesive sediment processes in an estuarine system: study case in Danshui River. *Environ.*  
644 *Model. Assess.* 15 (4), 261–271.

645 Gadel, F., Texier, H., 1986. Distribution and nature of organic matter in recent sediments of Lake  
646 Nokoué, Benin (West Africa). *Estuar. Coast Shelf Sci.*, 22, 767–784.

647 Gnohossou, P.M., 2006. La faune benthique d'une lagune ouest Africaine (le lac Nokoue au  
648 Bénin), diversité, abondance, variations temporelles et spatiales, place dans la chaîne trophique.  
649 Doctorat, *Institut National Polytechnique de Toulouse*, France, 184 p.

650 Halfman, J. D., & Scholz, C. A., 1993. Suspended sediments in Lake Malawi, Africa: a  
651 reconnaissance study. *Journal of Great Lakes Research*, 19(3), 499-511.

652 Hossain, S., Eyre, B.D., McKee, L.J., 2004. Impacts du dragage sur la concentration de  
653 sédiments en suspension en saison sèche dans l'estuaire de la rivière Brisbane, Queensland,  
654 Australie. *Sciences des estuaires, des côtes et des plateaux*, 61 (3), 539–545.

655 Hountondji, B., Codo, F., Dahounto, S., Gbaguidi, T., 2019. Flood Management in Urban  
656 Environment: Case of the Cotonou City in Benin. *LARHYSS Journal P-ISSN 1112-3680/E-*  
657 *ISSN 2521-9782*, 39, 333-347.

658 Jalil, A., Li, Y., Zhang, K., Gao, X., Wang, W., Khan, H.O.S., Acharya, K., 2019. Wind-induced  
659 hydrodynamic changes impact on sediment resuspension for large, shallow Lake Taihu,  
660 China. *International Journal of Sediment Research*, 34(3), 205-215.

661 Kari, E., Kratzer, S., José, M., Beltrán-Abaunza, E., Therese, H., Vaičiūtė, D., 2017. Retrieval of  
662 suspended particulate matter from turbidity – model development, validation, and application  
663 to MERIS data over the Baltic Sea, *International Journal of Remote Sensing*, 38:7, 1983-2003,

664 Kumar, A., Equeenuddin, S.M., Mishra, D.R., Acharya, B.C., 2016. Remote  
665 Monitoring of Sediment Dynamics in a Coastal Lagoon: Long-term Spatio-temporal Variability  
666 of Suspended Sediment in Chilika, *Estuarine, Coastal and Shelf Science*,

667 Kumar, K., Miral, M.S., Joshi, V., Panda Y.S., 2002. Discharge and suspended sediment in the  
668 meltwater of Gangotri Glacier, Garhwal Himalaya, India. *Hydrol. Sci. J.*, 47(4), 611–619.

669 Lalèyè, P., Villanueva, MC, Entsua-Mensah, M., Moreau, J., 2007. Une revue des ressources  
670 aquatiques vivantes dans les lagunes du golfe de Guinée avec un accent particulier sur la gestion  
671 des pêches. *Journal de zoologie afrotropicale*. Actes de la troisième Conférence internationale  
672 sur les poissons et les pêches en Afrique, Cotonou, Bénin, 10-14 novembre 2003, Numéro  
673 spécial, 123-136.

674 Le Barbé, L., Alé, G., Millet, B., Texier, H., Borel, Y., Gualde, R., 1993. Les Ressources  
675 en Eaux Superficielles de la République du Bénin. In : *Monographies Hydrologiques*, vol. 11,  
676 ORSTOM, Paris, ISBN : 2-7099-1168-X, p. 540

677 Llebot, C., Rueda, F.J., Solé, J., Artigas, M.L., Estrada, M., 2014. Hydrodynamic states in a wind-  
678 driven microtidal estuary (Alfacs Bay). *Journal of Sea Research*, 85, 263–276

679 Luettich, R.A., Harleman, D.R., Somlyody, L., 1990. Dynamic behavior of suspended sediment  
680 concentrations in a shallow lake perturbed by episodic wind events. *Limnology and*  
681 *Oceanography*, 35(5), 1050–1067

682 Macintosh, D.J., 1994. Aquaculture in coastal lagoons, Pp. 401-442, In: B. Kjerfve (ed.), Coastal  
683 Lagoon Processes. Amsterdam : *Elsevier*

684 Mama, D., 2010. Méthodologie et Résultats Du Diagnostic de L'Eutrophisation Du Lac Nokoue  
685 (Bénin) (Thèse de Doctorat), *Université de Limoges*, Limoges, France.

686 Mama, D., Deluchat, V., Bowen, J., Chouti, W., Yao, B., Gnon, B., Baudu, M., 2011.  
687 Caractérisation d'un Système Lagunaire en Zone Tropicale : Cas du lac Nokoué (Bénin). *Eur.*  
688 *J. Sci. Res.* 56 (4), 516–528.

689 Maxam, A.M., Webber, D.F., 2010. The influence of wind-driven currents on the circulation and  
690 bay dynamics of a semi-enclosed reefal bay, Wreck Bay, Jamaica. *Estuarine, Coastal and Shelf*  
691 *Science*, 87(4), 535–544.

692 McIntosh, P.C., 1990. Oceanographic data interpolation: objective analysis and splines. J.  
693 *Geophys. Res.* 95, 13529.

694 Moreina D., Claudia G., Gohin F., Cayocca F., Moira L., 2013. Suspended matter mean  
695 distribution and seasonal cycle in the Río de La Plata estuary and the adjacent shelf from ocean  
696 color satellite (MODIS) and in-situ observations; *Continental Shelf Research* 68 (2013) 51–66

697 Morel, Y., Chaigneau, A., Okpeitcha, V.O., Stieglitz, T., Assogba, A., Duhaut, T., Sohou, Z.  
698 2022. Terrestrial or oceanic forcing? Water level variations in coastal lagoons constrained by  
699 river inflow and ocean tides. *Advances in Water Resources*, 169, 104309.

700 Mulder, T., Syvitski P.M., Migeon S., Faugères J.C., Savoye B., 2003. Marine hyperpycnal  
701 flows: initiation, behavior and related deposits. A review, *Marine and Petroleum Geology*,  
702 Volume 20, Issues 6–8, Pages 861-882. <https://doi.org/10.1016/j.marpetgeo.2003.01.003>

703 Negusse, S.M., Bowen, J.D., 2010. Application of three-dimensional hydrodynamic and water  
704 quality models to study water hyacinth infestation in Lake Nokoué, Benin. In: *Estuarine and*  
705 *Coastal Modeling*. ASCE, pp. 409–427.

706 Neukermans, G., Ruddick, K., Loisel, H., Roose, P., 2012. Optimisation et contrôle qualité de  
707 Mesure de la concentration de particules en suspension à l'aide de mesures de turbidité.  
708 *Limnologie et océanographie méthodes* 10 : 1011 - 1023.

709 Niyonkuru, C., Lalèyè, P.A., 2010. Impact of acadja fisheries on fish assemblages in Lake  
710 Nokoué, Benin, West Africa. *Knowledge and Management of Aquatic Ecosystems*, (399), 05.

711 Okpeitcha, O.V., Chaigneau, A., Morel, Y., Stieglitz, T., Pomalegni, Y., Sohou, Z., Mama, D.,  
712 2022. Seasonal and interannual variability of salinity in a large West-African lagoon (Nokoué  
713 Lagoon, Benin). *Estuarine, Coastal and Shelf Science*, 264, 107689.



714 Ouillon, S., 2018. Why and how do we study sediment transport? Focus on coastal zones and  
715 ongoing methods, *Water*, 10, 390;

716 Parsons, J. D., Bush, J. W., & Syvitski, J. P., 2001. Hyperpycnal plume formation from riverine  
717 outflows with small sediment concentrations. *Sedimentology*, 48(2), 465-478.

718 Pérez-Ruzafa, A., Marcos, C., Pérez-Ruzafa, I.M., 2012. Fisheries in Coastal lagoons: An  
719 assumed but poorly researched aspect of the ecology and functioning of coastal lagoons.  
720 In *Estuarine, Coastal and Shelf Science*, 110, 15-31.

721 Picouet, C., Hingray, B., Olivry, J.C., 2001. Empirical and conceptual modelling of the  
722 suspended sediment dynamics in a large tropical African river: the Upper Niger river basin. *J.*  
723 *Hydrol.*, 250, 19–39.

724 Poff, N.L., Allan, J.D., Bain, M.B., Karr, J.R., Prestegard, K.L., Richter, B.D., Stromberg, J.C.,  
725 1997. The natural flow regime. *BioScience*, 47(11), 769-784.

726 Principaud, J.M., 1995. La pêche en milieu lagunaire dans le sud-est du Bénin. L'exemple de  
727 l'exploitation des acadjas (en danger) sur le lac Nokoué et la basse Sô. Dans : *Cahiers d'outre-*  
728 *mer*, 192, 48e année. Togo-Bénin, 519-546.

729 Qin, B., Hu, W., Chen, W., Fan, C., Ji, J., Chen, Y., Jiang, J., 2000. Studies on the hydrodynamic  
730 processes and related factors in Meiliang Bay, northern Taihu Lake, China. *Journal of Lake*  
731 *Sciences*, 12(4), 327–334

732 Spurgeon, J., 1999. The socioeconomic costs and benefits of coastal habitat rehabilitation and  
733 creation. *Mar. Pollut. Bull*, 37, 373–82.

734 Texier, H., Dossou, C., Colleuil, B., 1979. Étude de l'environnement lagunaire du domaine  
735 margino-littoral sud-béninois. Étude Hydrologique Préliminaire Du Lac Nokoué. *Bulletin de*  
736 *L'Institut de Géologie Du Bassin D'Aquitaine*, 25, 149–166.

737 Van Sickle, J., Beschta, R.L., 1983. Supply-based models of suspended sediment transport in  
738 streams. *Water Resour. Res.*, 19, 768–778.

739 Villanueva, M.C., Lalèyè, P., Albaret, J.J., Lae, R., de Morais, L.T., Moreau, J., 2006.  
740 Comparative analysis of trophic structure and interactions of two tropical lagoons. *Ecol. Model.*,  
741 197 (3), 461–477.

742 Walling, D.E., Webb, B.W., 1981. The reliability of suspended load data. In: *Erosion and*  
743 *Sediment Transport Measurement* (Proc. Florence Symp.), 177–194. IAHS Publ. 133. IAHS  
744 Press, Wallingford, UK.

745 Wentworth, C.K., 1922. A scale of grade and class terms for clastic sediments. *Journal of*  
746 *Geology*, 30, 377–392.

747 Weston, N.B., Neubauer, S.C., Velinsky, D.J., Vile, M.A., 2014. Net ecosystem carbon exchange  
748 and the greenhouse gas balance of tidal marshes along an estuarine salinity  
749 gradient. *Biogeochemistry*, 120, 163-189.

750 Wong, A.P.S., Johnson, G.C., Owens, W.B., 2003. Delayed-mode calibration of autonomous  
751 CTD profiling float salinity data by  $\chi$ -S climatology. *J. Atmos. Ocean. Technol.*, 20, 308–318.

752 Zandagba, J., Adandedji, F.M., Mama, D., Chabi, A., Afouda, A., 2016a. Assessment of the  
753 physico-chemical pollution of a water body in a perspective of integrated water resource  
754 management : case study of Nokoué lake. *J. Environ. Protect.*, 7, 656–669.

755 Zandagba, J., Moussa, M., Obada, E., Afouda, A., 2016b. Hydrodynamic modeling of Nokoue  
756 lake in Benin. *Hydrology* 3, 44.

757 Zavala, C., 2020. Hyperpycnal (over density) flows and deposits. *J. Palaeogeogr.* 9, 17.

758 Zăvoianu, I., 1996. Relationship between rainfall, slope runoff and erosion in the Valea Muscel  
759 Basin. *Geographical J.*, 48(2),113–120.

760 Zhu, G., Qin, B., Gao, G., 2005. Direct evidence of phosphorus outbreak release  
761 from sediment to overlying water in a large shallow lake caused by strong wind wave  
762 disturbance. *Chinese Science Bulletin*, 50(6), 577–582.

763